

***In vivo* multiphoton fluorescence correlation spectroscopy to quantify cerebral blood flow with high spatiotemporal resolution**

Cerebral blood flow (CBF) measurements provide critical information about physiological and pathological processes within the central nervous system (CNS). The complex microvascular network plays a fundamental role within the CNS, where neuronal activity regulates the flow of nutrients. Understanding blood flow dynamics with high spatial and temporal resolution is essential to understanding the role of vascular dysfunction in a variety of pathological processes. Using multiphoton *in vivo* fluorescence correlation spectroscopy (FCS), blood flow rates can be determined at individual pixels with sub-micron resolution.

Free Webinar
November 12, 2020
11 am EST

Sponsored by:



Provided by:

WILEY

MR. ADAM J REID (Orcid ID : 0000-0003-1752-3302)

DR. ALESSANDRO FARONI (Orcid ID : 0000-0003-4435-6423)

Article type : Special Issue Article

PERIPHERAL NERVE REGENERATION FOLLOWING INJURY IS ALTERED IN MICE LACKING P2X7 RECEPTOR

Valerio Magnaghi¹, Sarah Martin², Patrick Smith², Luke Allen², Vincenzo Conte³, Adam J Reid^{2,4} and Alessandro Faroni²

¹ *Department of Pharmacological and Biomolecular Sciences, Università degli Studi di Milano, Milan, Italy*

² *Blond McIndoe Laboratories, Division of Cell Matrix Biology and Regenerative Medicine, School of Biological Sciences, Faculty of Biology Medicine and Health, University of Manchester, Manchester Academic Health Science Centre, Manchester, M13 9PL, UK*

³ *Department of Biomedical Sciences for Health, Università degli Studi di Milano, Milan, Italy*

⁴ *Department of Plastic Surgery & Burns, Wythenshawe Hospital, Manchester University NHS Foundation Trust, Manchester Academic Health Science Centre, Manchester, M23 9LT, UK*

Correspondence: Dr. Alessandro Faroni, as above.

e-mail: alessandro.faroni@manchester.ac.uk

Running title: Nerve regeneration in P2X₇ KO mice

Total pages: 30 Figures: 7

Number of words in the manuscript: 8794

This article has been accepted for publication and undergone full peer review but has not been through the copyediting, typesetting, pagination and proofreading process, which may lead to differences between this version and the [Version of Record](#). Please cite this article as [doi: 10.1111/EJN.14995](https://doi.org/10.1111/EJN.14995)

This article is protected by copyright. All rights reserved

Number of words in the Abstract: 213

Number of words in the Introduction: 421

Keywords: myelin, unmyelinated fibers, Schwann cell, axon, cytokine

Abstract

Peripheral nerve injuries are debilitating, and current clinical management is limited to surgical intervention, which often lead to poor functional outcomes. Development of pharmacological interventions aimed at enhancing regeneration may improve this. One potential pharmacological target is the P2X purinergic receptor 7 (P2X7R) expressed in Schwann cells, which is known to play a role during the development of the peripheral nerves. Herein, we analysed differences in regeneration between genetically engineered P2X7 knockout mice and wild-type controls, using *in vivo* and *ex vivo* models of peripheral nerve regeneration. We have found that the speed of axonal regeneration is unaltered in P2X7 knockout mice, nevertheless regenerated P2X7 knockout nerves are morphologically different to wild-type nerves following transection and immediate repair. Indeed, the detailed morphometric analysis at 4 and 8 weeks after injury showed evidence of delayed remyelination in P2X7 knockout mice, compared to the wild type controls. Furthermore, the Wallerian degeneration phase was unaltered between the two experimental groups. We also analysed gene expression changes in the dorsal root ganglia neurones as a result of the peripheral nerve injury, and found changes in pathways related to pain, inflammation and cell death. We conclude that P2X7 receptors in Schwann cells may be a putative pharmacological target to control cell fate following injury, thus enhancing nerve re-myelination.

Introduction

Peripheral nerve injuries, occurring as a result of trauma to upper and lower limbs, are common and debilitating. The most severely affected patients may face permanent disability, chronic pain, and psychological challenges. Current treatments, merely limited to surgical repair, are ineffective and lead to poor functional recovery (Zochodne, 2012). There are no pharmacological interventions that can improve regeneration and repair, however several molecules and receptors, targeting mainly Schwann cells, have been suggested as potential candidates for pharmaceutical therapies (Magnaghi *et al.*, 2009). These pharmacological strategies to enhance nerve regeneration include the use of neurosteroids, neurotransmitters and other small molecules (Martinez de Albornoz *et al.*, 2011). Indeed, research has shown that receptors for neurotransmitters such as γ -aminobutyric acid (GABA), Acetylcholine (Ach), and adenosine triphosphate (ATP), are able to modulate physiological parameters in Schwann cells, which may be exploited to improve peripheral nerve regeneration outcomes (Faroni *et al.*, 2014a; Faroni *et al.*, 2014b; Uggenti *et al.*, 2014). Mice lacking receptors for GABA, Ach and ATP have shown an altered peripheral nerve development, that results in specific peripheral nervous system (PNS) phenotypes (Magnaghi *et al.*, 2008; Faroni *et al.*, 2014b; Uggenti *et al.*, 2014).

The P2X purinergic receptor 7 (P2X7R) is a plasma membrane ligand-gated ion channel operated by ATP. In Schwann cells, these receptors bind ATP released from dorsal root ganglia (DRG) and axons in an activity-dependent manner, however the effects of ATP on downstream purinergic signalling pathways involved in peripheral nerve regeneration, myelination and function are largely unknown (Stevens *et al.*, 1998; Fields & Stevens, 2000; Stevens & Fields, 2000). Previous work by our group has shown that P2X7R is expressed predominantly in myelinating Schwann cells and that, during development, lack of P2X7R causes Schwann cells to commit to a non-myelinating phenotype (Faroni *et al.*, 2014b). These results were obtained by studying P2X7R knockout mice developed by GlaxoSmithKline (GSK) (Chessell *et al.*, 2005), however another mouse strain with ablation of P2X7R was developed by Pfizer Inc. (Solle *et al.*, 2001), and the two models have been reported to possess similar, although not identical, phenotypes (Sim *et al.*, 2004). In the current study, we aimed to confirm the PNS phenotype, we previously observed in the GSK mouse model, in Pfizer's mice strain. Moreover, we aimed to determine whether P2X7R affects the speed of degeneration, regeneration and myelin formation following nerve transection.

This will be done through characterising the differences between genetically engineered P2X7R

knock out (KO) mouse model, and wild type (WT) controls, in *ex vivo* and *in vivo* models of peripheral nerve injury and repair.

Accepted Article

Materials and Methods

Experimental mice and surgical procedures

All animal experiments were performed in accordance with the UK Animals (Scientific Procedures) Act, 1986. Pfizer P2X7 KO mice (B6.129P2-P2rx7^{tm1Gab}/J) were acquired from The Jackson Laboratory, US (Solle *et al.*, 2001). C57BL/6 mice obtained from the Biological Service Facility of the University of Manchester were used as WT controls. All mice were 3-4 month old males. For surgical transection, animals were anaesthetised with isoflurane and the sciatic nerves were transected. Immediately following transection the sciatic nerves were repaired with 11-0 sutures under an operating microscope (Leica, United Kingdom). For the non-repair group, the proximal and distal stumps of sciatic nerve were sutured to an adjacent muscle. One week after the axotomy and no repair surgery, mice underwent terminal anaesthesia with carbon dioxide (CO₂) and cervical dislocation. The lumbar 4 and 5 DRGs were removed via cutting of the central and peripheral branch, close to the ganglia. The DRGs were harvested from the injured (Inj) and the contralateral control side (Ctrl) in all mice (P2X7 KO and WT). Samples were collected with n=5 for the four groups and stored at -40°C until real time PCR analyses. For the injury and repair experiments, tissues were collected at 1 and 2 weeks and processed for immunohistochemistry (n=5). Furthermore, we performed long term studies at 4 and 8 weeks survival for morphometric analyses through transmission electron microscopy analyses (n=4).

Genotyping

Ear clippings from KO and WT animals were lysed for 2 hours at 55°C and DNA was isolated by adding phenol:chloroform:isoamyl alcohol solution (25:24:1, Sigma-Aldrich, UK). Lysis buffer was: 100mM NaCl, 10mM Tris Buffer, 1mM EDTA, 1% SDS, 0.1 mg/ml Proteinase K (all from Sigma-Aldrich). For polymerase chain reaction (PCR), each well contained 1µl of extracted DNA and 9µl master mix (5X Green GoTaq Flexi buffer, MgCl₂ 2mM, dNTPs 0.2 mM, primers mix 0.5µM each, GoTaq DNA polymerase 5U/ µl, Promega, Southampton, United Kingdom). Primers were obtained from Sigma and sequences were as follows: WT allele: 5'-TGG ACT TCT CCG ACC TGT CT-3' and 5'-TGG CAT AGC ACC TGT AAG CA-3'; KO allele: 5'-CTT GGG TGG AGA GGC TAT TC-3' and 5'-AGG TGA GAT GAC AGG AGA TC-3'. The PCR protocol used can be found on the Jackson Laboratories website, and it involved 28 cycles of 94°C for 15 seconds, annealing at 50°C for 15 seconds, and extension at 72°C for 10 seconds; followed by 72°C of final extension for 2 minutes and hold at 4°C. Following PCR, samples were loaded onto

a 1.5% agarose gel and were run at 80V for 1.5 hours before analysis with an AlphaImager 2200 gel documentation system (Alpha Innotech/Proteinsimple, Santa Clara, California).

Western Blot

Sciatic nerves were first homogenised using a tissue ruptor (Qiagen, Manchester, UK) and left to lyse on ice in lysis buffer for 30 minutes. Samples were then freeze/thawed and centrifuged at 13,000g, 4°C, for 15 minutes (IEC CL31R Multispeed; Fisher Scientific, Loughborough, United Kingdom) before separating the supernatant from the pellet. Supernatant protein concentration was determined using the Bio-Rad detergent-compatible protein assay (Bio-Rad Laboratories, Hemel Hempstead, United Kingdom) and standard curve of bovine serum albumin (BSA; Sigma-Aldrich) standards, and a spectrophotometer (Asys UVM340 Microplate Reader; Bichrom, Cambridge, United Kingdom). 10µg of protein from each sample were mixed with loading buffer (2X buffer: Tris-HCl 100mM, pH 6.8, SDS 4% (w/v), bromophenol blue 0.2% (w/v), glycerol 20% (v/v), β-mercaptoethanol 200mM; Sigma-Aldrich), and boiled at 100°C for 3 minutes, followed by centrifugation at 13,000g at room temperature for 1 minute. Samples were loaded onto a 10% polyacrylamide gel (40% acrylamide 29:1; Sigma-Aldrich) with protein marker (ColorPlus prestained protein marker, 8-175 kDa; New England Biolabs, Hitchin, United Kingdom) and ran for 90-120 minutes at 80-120V. Gels were transferred onto a nitrocellulose membrane (Amersham Hybond-ECL; GE Healthcare, Little Chalfont, United Kingdom) with a Bio-Rad wet transfer apparatus (transfer buffer: Tris-base 25mM, glycine 192mM, methanol 20% (v/v) at 80V for one hour. To confirm protein transfer membranes were then treated with ponceau red (ponceau 0.1% (w/v), acetic acid 0.5% (v/v)). Membranes were blocked in 5% (w/v) skimmed milk in tris-buffered saline-Tween (TBST; Tween-20 0.5% (v/w), NaCl 140mM, Tris 10mM, pH 7.5) for 30-60 minutes and incubated in primary antibodies overnight at 4°C on a shaker. The following day membranes were washed for 30 minutes in TBST, incubated in horseradish peroxidase (HRP)-conjugated secondary antibodies at room temperature for one hour, and washed for 30 minutes in TBST. Primary antibodies were used at the following dilutions: anti-P0, 1:200 (Abcam, UK); anti-MBP, 1:200 (Millipore, UK); anti-MAG, 1:200 (Cell Signalling Technologies, UK). Rabbit secondary -HRP antibodies were used 1:500 (Cell Signalling Technologies, UK). Membranes were treated with pico- or femtochemiluminescence mixes (SuperSignal West pico/femto chemiluminescent substrate; Fisher Scientific) for five minutes for signal detection. Luminescent bands were imaged using a Kodak Image Station 4000mm PRO. Densitometry

analysis was performed in Image J (version 1.47f, NIH, USA). Bands were normalised to the housekeeping protein β -tubulin data was expressed as the percentage versus the WT control.

Immunohistochemistry

Following overnight fixation in 4% (w/v) paraformaldehyde (PFA) at 4°C, sciatic nerves were cryoprotected in 15% (w/v) sucrose in phosphate buffered saline (PBS) which was replaced daily for 3 days. Nerves were embedded in optimal cutting temperature embedding matrix (Raymond A Lamb, Eastbourne, United Kingdom), and stored at -80°C until further processing. Nerves were then sliced into 15 μ m longitudinal sections using a cryostat (OTF; Bright Instruments, Cambridgeshire, United Kingdom) set at -20°C. Slices were dried overnight at 37°C, before permeabilisation in 0.2% (v/v) Triton X-100 in PBS for 1 hour at room temperature, and a further two washes in PBS for 5 minutes. Sections were then blocked in 5% blocking serum (Normal Goat Serum, Sigma) diluted 1:100 in antibody diluent (0.03% (v/v) Triton, 0.10% (w/v) BSA, 0.10% (w/v) sodium azide) for 1 hour at room temperature. Sections were then incubated in a rabbit primary antibody labelling neurofilament 200 (NF200, Sigma-Aldrich) overnight at 4°C. After incubation, sections were washed in PBS for 5 minutes twice, incubated in Alexa-488 labelled anti-rabbit secondary antibody raised in goat (Thermo Scientific, UK) for 2 hours at room temperature and in dark conditions, and then washed twice in PBS for 5 minutes. Finally, coverslips were fitted to the slides using Vectashield with 4',6-diamidino-2-phenylindole (DAPI) H-1200 (Vector Laboratories, Peterborough, United Kingdom). Fluorescence microscopy analysis was performed with an Olympus BX60 fluorescence microscope, and images were recorded in Image ProPlus v 6.0 (Media Cybernetics, Rockville, Maryland). Tiled images were merged using Photoshop CS6 (Adobe).

Explant culture as Wallerian Degeneration (WD) Model

Following terminal anesthesia using carbon dioxide (CO₂) and cervical dislocation, approximately a 10 millimeters (mm) segment of the sciatic nerves (from both legs) were removed from both P2X7 KO and WT mice (n=3). Three nerve segments from each group nerve were frozen immediately in liquid nitrogen to ensure Wallerian degeneration could not occur. These samples are referred to as time zero (T0). Contralateral KO and WT sciatic nerves were divided into 1-2mm long sections and cultured as floating nerve explants in Dulbecco's modified eagles medium (DMEM, Sigma), containing 10% (v/v) fetal bovine serum (FBS, Labtech), 2% (v/v) L-glutamine

(sigma) and 1% (v/v) penicillin-streptomycin (p-s, Sigma). The cultures were maintained at 37°C in a humidified atmosphere containing 5% Carbon dioxide (CO₂) for 72 hours to recapitulate Wallerian degeneration *ex vivo*. After culture, samples were then frozen using liquid nitrogen and stored in a -40°C freezer until real time PCR analyses. These samples are referred to as T72 (time point 72 hours).

Real-Time Quantitative Polymerase Chain Reaction

The RNeasy lipid tissue mini kit (Qiagen) was used for the extraction of RNA from the sciatic nerves and DRG samples. Tissues were homogenized using the Qiagen Tissue Ruptor (for nerves) or mortar and pestle (DRG). Chloroform was then added and the tissue was centrifuged at 12,000 x g for 15 minutes to separate the nucleic acids in the aqueous phase. Following ethanol addition, the mixture was applied to RNeasy spin column to purify RNA and get rid of contaminants. The concentration of RNA obtained from both tissues types was then determined by the measuring the absorbance at 260nm using a Nanodrop-1000 spectrophotometer (Thermo Scientific). The extracted RNA was reverse transcribed using the RT² First Strand Kit (QIAGEN) and a PTC-200 Peltier Thermal Cycler (MJ Research) according to manufacturer instructions. Either 100ng (DRG) or 140ng (nerves) of RNA were reverse transcribed. Primers for RT-PCR are listed in Table 1. PCR reactions were performed with a Corbett Research thermocycler, using ad RT² SYBR Green kit (QIAGEN, UK), and data was analysed with RotorGene-6000 series software (version 1.7). The PCR conditions were set to: 1 step at 95°C for 10 minutes to activate the HotStart DNA Taq Polymerase, followed by 40 cycles of 15 seconds at 95°C, 30 seconds at 55°C and 30 seconds at 72°C, where the fluorescence data was collected. The protocol was terminated with a melting curve program of 95°C for 1 minute, 65°C for 2 minutes, and gradual change from 65°C to 95°C, with a 1°C increase at each step. Data was analysed via the $\Delta\Delta C_t$ method, and normalised for the housekeeping gene (18s) and the control groups (uninjured control and T0 control nerves).

Table 1 Table of primers used in real time-PCR studies

| Gene | Primer Sequence (5'-3') | PL (bp) | Reference |
|-------|--------------------------|---------|-------------------------------|
| CASP2 | FW: CCACAGATGCTACGGAACA | 99 | (Hanoux <i>et al.</i> , 2007) |
| | RV: GCTGGTAGTGTGCCTGGTAA | | |
| CASP3 | FW: TGCAGCATGCTGAAGCTGTA | 150 | (Gesing <i>et al.</i> , 2015) |

| | | | |
|--------------|--|-----|---------------------------------------|
| ATF3 | RV: GAGCATGGACACAATACACG FW: GCTGCCAAGTGTCGAAACAAG | 331 | (Allen-Jennings <i>et al.</i> , 2001) |
| GAP43 | RV: CAGTTTTCCAATGGCTTCAGG FW: TGTGGGAGTCCACTTTCCTC | 64 | (Namsolleck <i>et al.</i> , 2013) |
| NGF-B | RV: GAACGGAACATTGCACACAC FW: CCAGTGAAATTAGGTCCTCTG | 143 | (Namsolleck <i>et al.</i> , 2013) |
| GAL | RV: CCCTTGGCAAAACCTTTATTGGG FW: TGGAGGAAAGGAGACCAGGAAG | 100 | (He <i>et al.</i> , 2005) |
| NFkB | RV: GCCTCTTTAAGGTGCAAGAAACTG FW: CTACGGAAGTGGGCAAATGT | 145 | (Nagajyothi <i>et al.</i> , 2012) |
| TNFa | RV: TCGAAATCCCCTCTGTTTTG FW: CCGATGGGTTGTACCTTGTC | 77 | (Cunningham <i>et al.</i> , 2002) |
| 18S | RV: GTGGGTGAGGAGCACGTAGT FW: CTGCCCTATCAACTTTCGATGGTAG | 100 | (Faroni <i>et al.</i> , 2014b) |
| MAG | RV: CCGTTTCTCAGGCTCCCTCTC FW: CACCTTCTCGGAGCACAG | 78 | (Faroni <i>et al.</i> , 2014b) |
| MBP | RV: GTTCTGCCACCACTTCC FW: AGGACTCACACACGAGAACTACCC | 121 | (Faroni <i>et al.</i> , 2014b) |
| PMP22 | RV: GGTGTTCGAGGTGTCACAATGTTC FW: CGGTTTTACATCACTGGATTCTTC | 98 | (Faroni <i>et al.</i> , 2014b) |
| P0 | RV: TTGACATGCCACTCACTGT FW: TGACAACGGCACTTTCACA | 118 | (Faroni <i>et al.</i> , 2014b) |
| BDNF | RV: TCCCAACACCACCCATA FW: GGTATCCAAAGGCCAACTGA | 183 | (Faroni <i>et al.</i> , 2014b) |
| | RV: CTTATGAATCGCCAGCCAAT | | |

Transmission Electron Microscopy

Following terminal anaesthesia and cervical spine dislocation, mice were perfused transcardially with 2% paraformaldehyde and 2% glutaraldehyde in sodium cacodylate buffer (0.1M, pH 7.3) for fixation. The sciatic nerves were then harvested and immersed in the same fixative solution overnight at 4°C. Samples were postfixed in 2% OsO₄ (Sigma-Aldrich), washed in distilled water, stained with 2% aqueous uranyl acetate, dehydrated in graded alcohol, and embedded in Epon-Araldite resin. Ultrathin sections (ca. 70–80 nm) of the fixed sciatic nerves were collected on formvar coated single slot grids and counterstained with lead citrate, then examined with a Zeiss EM 10 electron microscope (Oberkochen, Germany). For morphological analysis, more than 25% of the total cross-sectional area of each nerve (corresponding to at least 25% of the total nerve cross-sectional area, about 90-100 fields) were randomly selected using a systematic random-square sampling method throughout the entire nerve profile (Mayhew & Sharma, 1984) and Image

Accepted Article

Pro-Plus 6.0. The measurement of myelinated fibers (at least 1,500 fibers/animal), myelin thickness, G-ratio (ratio between inner axonal diameter and total outer diameter of the fiber) and irregular fibers [index of circularity (IC), calculated as squared fiber perimeter/4 π fiber area, <0.75] were assessed. The number of Remak bundles, number of unmyelinated axons in each bundle, number of single unmyelinated and myelinated axons were counted. Data were expressed per unit of surface area (100 μm^2) \pm standards error of the mean (SEM).

Statistical Analysis

All statistical analyses were performed using GraphPad Prism (version 8.2.1 for Mac; GraphPad Software, San Diego, California). Statistical significance was evaluated by two-tailed unpaired t-tests or two-way analysis of variance (ANOVA). Results were considered significant at $P < 0.05$.

Results

Confirming PNS phenotype in Pfizer's P2X₇R knockout mouse strain

Pfizer's P2X₇ knockout (KO) mice (3 month-old males) were sourced from The Jackson Laboratory (B6.129P2-P2rx7^{tm1Gab/J}), and C57BL/6 wild type (WT) were used as controls. Firstly, we demonstrated the ablation of P2X₇R by using specific primer sequences. Indeed, PCR analyses performed on tail biopsies or ear punches confirmed that the experimental mice express the KO sequence (280bp), and not the WT sequence (363bp). All control mice express the WT P2X₇ sequence (363bp), and heterozygote mice express both the WT and KO sequence (280bp and 363bp, Figure 1A).

Since significant differences have been reported in GSK and Pfizer's P2X₇ KO mice (Sim *et al.*, 2004), we proceeded to confirm the PNS phenotype we previously reported in GSK mice (Faroni *et al.*, 2014b), in the newly acquired Pfizer model. Interestingly, we observed significant reduction of the protein levels of the main peripheral myelin proteins protein zero (P0, ****P < 0.0001), myelin basic protein (MBP, *P < 0.05) and myelin associated glycoprotein (MAG, **P < 0.01) using western blot analyses (Figure 1B). Moreover, transmission electron microscopy analyses confirmed the altered morphology of P2X₇ KO mice, which feature a significantly higher number of Remak bundles (**P < 0.001), containing a higher number of unmyelinated axons (**P < 0.001, Figure 1C). Albeit not statistically significant, P2X₇R knockout mice showed a reduced myelinated/unmyelinated axon ratio compared to WT controls, but the overall myelin thickness was unaltered. Finally, the percentage of irregular fibers, with circularity index (IC) lower than 0.75, was significantly higher in P2X₇R knockout mice compared to WT controls (*P < 0.05).

Gene expression changes in DRG neurons following nerve transection

Given that peripheral nerve injury is accompanied with profound changes in gene expression at the level of the DRG neurons (Martin *et al.*, 2019), we investigated if some of these changes could be affected by the absence of P2X7R. We analysed the expression levels for markers of cell death, inflammation, survival and regeneration in DRG by real-time PCR, 1 week after peripheral nerve transection and no repair (Figure 2A). Peripheral nerve injury caused an increase in caspase 2 (CASP2) gene expression level in DRG from both WT (ns) and P2X7 KO (**P < 0.01) mice, as well as an increase in caspase 3 (CASP3, ****P < 0.0001 WT; ***P < 0.001 P2X7 KO) gene expression levels (Figure 2B).

Markers of inflammation were also upregulated in DRG after nerve transection in both WT and P2X7R KO mice (Figure 2C). Indeed, nuclear factor kappa-light-chain-enhancer of activated B cells (NFkB) levels were marginally increased after injury in WT mice (ns), whereas in P2X7 KO the increase was statistically significant (**P < 0.01). Conversely, tumor necrosis alpha (TNF α) expression levels were significantly increased after injury in WT mice (*P < 0.05), but only marginally increased in P2X7 KO (ns).

Furthermore, we analysed markers of survival, nerve function and nociception such as Activating Transcription Factor 3 (ATF3), Growth Associated Protein 43 (GAP43), Nerve Growth Factor (NGF) and galanin (GAL, Figure 2D). Nerve transection caused a significant increase in the expression levels of ATF3 in the DRGs of both WT (****P < 0.0001) and P2X7 KO mice (***P < 0.001). Similarly, levels of GAP43 were significantly increased in WT (**P < 0.01) and P2X7 KO (***P < 0.001) DRGs after injury. NGF was also upregulated in DRG after injury in both WT (**P < 0.01) and KO (*P < 0.05) groups. Overall, no major differences in the expression levels were observed between the WT and KO mice. Nevertheless, we found increased expression levels of the neuropeptide GAL in both WT (****P < 0.0001) and P2X7 KO DRGs (****P < 0.0001) after injury, and GAL expression levels were significantly higher in injured P2X7 KO DRGs compared to injured WT (***P < 0.001)

Degeneration and Regeneration speed are not affected by P2X₇R absence

To assess the effect of P2X7R ablation on the efficacy of nerve regrowth we performed a sciatic nerve transection with immediate repair, and performed histological analyses on longitudinal nerve sections 1 and 2 weeks after survival (Figure 3A). One week after the injury and repair, evidence of growing axonal cones could be observed (neurofilament 200 staining, NF200, green) at the injury/repair site (red line); whereas in the distal stump the distribution of the axonal debris

suggested ongoing Wallerian degeneration, without major differences between the WT and P2X7 KO groups (Figure 3B). Following 2 weeks survival, NF200 staining (green) showed complete regeneration of newly formed axons within the distal stump in both experimental groups (Figure 3C).

To confirm that WD is not affected by the absence of P2X7R, we performed gene expression analyses in an *ex vivo* model of WD. We chose an *ex vivo*, rather than *in vivo* model in order to minimise the systemic effects of P2X7R ablation, and focus on the effects of P2X7R removal mainly in Schwann cells. Sciatic nerves were collected from WT and P2X7 KO mice, and cultured as explants for 72 hours to recapitulate WD *in vitro*.

We started by analysing the levels of the main myelin proteins in the peripheral nerves: MAG, MBP, PMP22 and P0. Freshly isolated sciatic nerves (T0) from P2X7 KO mice expressed significantly higher levels of MAG (**P < 0.01, Figure 4A). Following 72 hours of *in vitro* WD (T72), MAG expression levels were significantly decreased in both WT and P2X7 KO nerves (****P < 0.0001, Figure 4A). Basal MBP gene expression levels were similar in WT and P2X7 KO (ns, Figure 4B), and following 72 hours of degeneration *in vitro* MBP expression was significantly decreased in both (***P < 0.001 for WT, and ****P < 0.0001 for P2X7 KO respectively, Figure 4B). At T0, P2X7 KO nerves expressed significantly higher levels of PMP22 compared to WT controls (***P < 0.001, Figure 4C); at T72, PMP22 gene expression levels were significantly decreased (****P < 0.0001, Figure 4C). P0 expression levels were marginally higher at T0 in P2X7 KO compared to WT (ns, Figure 4D), and at T72 there was a significant decrease of expression levels in both WT (**P < 0.01) and KO (****P < 0.0001) nerves (Figure 4D).

We then analysed expression levels of neurotrophic factors involved in WD such as nerve growth factor (NGF) and brain derived neurotrophic factor (BDNF). BDNF expression levels were marginally higher in P2X7 KO compare to WT, although this was not statistically significant (ns, Figure 4E). In both experimental groups, BDNF levels were greatly upregulated after *ex vivo* degeneration (****P < 0.0001, Figure 4E). No significant differences were observed in BDNF expression between P2X7R KO and WT at T72. Similarly, NGF levels were higher in P2X7 KO nerves compare to WT (ns, Figure 4F), and the expression of NGF was significantly increased in both groups after WD (****P < 0.0001), with no significant differences between the two (ns, Figure 4F).

Finally, we analysed gene expression changes of apoptotic genes such as Caspase-2 (CASP2) and Caspase-3 (CASP3). CASP2 levels were similar in P2X7 KO nerves compared to WT at both T0

and T72 (ns), with only a marginal but not significant increase between the two time points within each group (ns, Figure 4G). CASP3 expression was marginally lower in P2X7 KO compared to WT nerves at T0 (ns), and significantly increased in both groups (****P < 0.0001), without significant differences between WT and KO (Figure 4H).

Re-myelination following nerve regeneration is delayed in P2X7 KO mice

To assess if the absence of P2X7R affects the capability of Schwann cells to remyelinate regenerating axons, we performed morphometric analyses of the distal stumps of regenerated nerves from WT and KO 4 and 8 weeks after the injury. The light and transmission electron microscopy analyses showed a different regenerating phenotype in peripheral nerves from injured P2X7R KO mice compared to control animals (WT). At 4 weeks after the injury, the P2X7R KO nerves had a significantly lower number of Remak bundles compared to WT (***P < 0.001, Figure 5A). By week 8, the number of Remak bundles in the P2X7 KO nerves had increased significantly (***P < 0.001) compared to 4 weeks P2X7R nerves, and was similar to WT nerves (ns). At 4 weeks, the Remak bundles in the injured KO nerves contained a significantly lower number of unmyelinated axons compared to WT (***P < 0.001, Figure 5B), and this did not change at the 8 weeks time point (ns), where the unmyelinated axons within the KO Remak were still lower compared to 8 weeks WT controls (***P < 0.001, Figure 5B). The effect at 4 weeks was also confirmed in transmission electron microscopy images (Figure 6A), in which the unmyelinated axons appeared lower in KO nerves compared to WT. At 4 weeks after injury we also found a higher number of single unmyelinated axons (not contained within a Remak bundle) in P2X7 KO nerves compared to WT (***P < 0.001, Figure 5C). The number of single unmyelinated axons significantly increased in P2X7 KO nerves after further 4 weeks (***P < 0.001), although at 8 weeks the number of single unmyelinated axons was significantly higher in WT nerves compared to P2X7 KO (*P < 0.05, Figure 5C). This was further shown in transmission electron microscopy images (Figure 6B) still confirming a decrease in single unmyelinated fibers. Despite these changes, the total number of unmyelinated axons (both in Remaks and singles) was lower in P2X7 KO nerves compared to WT at both time points (***P < 0.001), while a weak but significant increase was observed in P2X7 KO between 4 and 8 weeks after injury (***P < 0.001, Figure 5D). Interestingly, transmission electron microscopy images evidenced a particular structure formed by a Schwann cell, enveloping some unmyelinated axons, and surrounding a myelinated fiber (Figure 6C). At 4 weeks after the injury the ratio between myelinated and unmyelinated axons was significantly higher in P2X7 KO mice compared to WT, (***P < 0.001,

Figure 5E); this ratio significantly increased ($***P < 0.001$) at the 8 weeks time point (Figure 5E). The overall number of myelinated axons was significantly lower in P2X7 KO nerves compared to WT, at both time points considered ($***P < 0.001$, Figure 5F), although it significantly increased in P2X7 KO between 4 and 8 weeks after the injury ($***P < 0.001$, Figure 5F). Myelin thickness was significantly lower in P2X7 KO nerves compared to WT at 4 weeks ($***P < 0.001$, Figure 5G), and rose significantly in P2X7 KO at 8 weeks, when compared to WT ($***P < 0.001$, Figure 5G). Interestingly, myelin thickness augmented significantly in P2X7 KO nerves comparing the 4 to the 8 weeks time point ($***P < 0.001$, Figure 5G; see also Figure 6A and 6B). Conversely, in P2X7 KO nerves the G-ratio was higher than WT at 4 weeks after injury and lower than WT after 8 weeks, with a significant decrease between the 2 time points ($***P < 0.001$, Figure 5H). Finally, an increase in the percentage of irregular fibers (IC lower than 0.75) was found in P2X7 KO nerves at 4 weeks (65% in KO vs 47% in WT), although this difference flattened at 8 weeks (P2X7 KO nerves 76% vs WT 79%).

Discussion

Pharmaceutical therapies for peripheral nerve injury are currently unavailable. A large number of pharmaceutical targets have been proposed as promising candidates for the development of novel therapies for peripheral nerve regeneration. In particular, extensive research has been focusing on neurotransmitters such as GABA, ATP and Ach, and their receptors, as systems to be targeted. In previous work, we have shown how GABA receptors play important roles in determining the fate of Schwann cells during development (Magnaghi *et al.*, 2009; Faroni & Magnaghi, 2011). Indeed, mice lacking GABA-B1 receptors in the whole organism (Magnaghi *et al.*, 2008), or selectively in Schwann cells (Faroni *et al.*, 2014a), showed an altered phenotype of peripheral nerve morphology and phenotype, highlighting the importance of GABA-B1 receptors for the SC commitment to a non-myelinating phenotype. This was also confirmed with *in vitro* cultures of SC and DRG neurons from GABA-B1 knockout animals (Faroni *et al.*, 2019). Treatment with GABA ligands modulates the production and release of neurotrophins in SC *in vitro* (Faroni *et al.*, 2013a), and promotes nerve regeneration in a sciatic nerve lesion model *in vivo* (Magnaghi *et al.*, 2014). Ach signaling has also been extensively associated with the regulation of myelination, and particularly more recently with the regulation of Schwann cell physiology during development and remyelination following injury (Fields *et al.*, 2017). Indeed, Schwann cells express several muscarinic receptors, with M2 being specifically important for Schwann cell proliferation and

myelin formation (Loreti *et al.*, 2006; Loreti *et al.*, 2007; Uggenti *et al.*, 2014). Similarly, purinergic receptors for ATP have been identified in several glial cells, including Schwann cells, where they take part in several neuron-glia interactions that are fundamental for glial cell pathophysiology (Fields & Stevens, 2000; Fields & Burnstock, 2006; Verkhratsky *et al.*, 2009; Lecca *et al.*, 2012). Indeed, Schwann cells located along axon segments respond to ATP and other neurotransmitters released by axons during electrical stimulation, which in turn may affect Schwann cell proliferation, differentiation, and myelination (Stevens *et al.*, 1998; Fields & Stevens, 2000; Stevens & Fields, 2000; Fields & Stevens-Graham, 2002; Stevens *et al.*, 2002; Fields & Burnstock, 2006; Fields *et al.*, 2017). Furthermore, several cellular mechanisms for ATP release, including P2X₇R, have been identified in non-neuronal cells (Fields, 2011).

In a previous study, we demonstrated that P2X₇ receptors localise mainly in myelinating Schwann cells in the PNS. Moreover, we showed that peripheral nerves from P2X₇ KO mice possess an altered molecular and morphological phenotype, suggesting a key role for P2X₇R to determine Schwann cell fate during development (Faroni *et al.*, 2014b). This peculiar phenotype results was described in the P2X₇ KO mice developed by GSK, (Chessell *et al.*, 2005), however Pfizer developed a similar knockout model (Solle *et al.*, 2001), which showed similar but not identical characteristics (Sim *et al.*, 2004). For this reason, in the current work we repeated some of the initial characterisation of the peripheral nerves phenotype studied in GSK P2X₇ KO (Faroni *et al.*, 2014b), also in the Pfizer mice developed by Solle *et al.* (Solle *et al.*, 2001). As in the GSK P2X₇ KO model (Faroni *et al.*, 2014b), Pfizer P2X₇ KO mice also showed reduced expression of myelin proteins P0, MBP and MAG, as well as featuring the main morphometric properties of the GSK model (increased number of Remak and unmyelinated axons, as well as irregular fibers).

Furthermore, in this study, we focused on the role of P2X₇ receptor during injury and repair. Using *ex vivo* and *in vivo* models of nerve regeneration, we found that the absence of P2X₇R does not affect the degenerative phase (Wallerian degeneration) that follows nerve injury and does not influence the speed of axonal regeneration. Nevertheless, EM studies showed that re-myelination is delayed in P2X₇ KO mice, suggesting a role for P2X₇R in the determination of the myelinating phenotype in injury and repair, in the same way it does during development. Indeed, KO mice showed a lower number of myelinated axons compared to WT at both 4 weeks and 8 weeks after the injury and repair. The number of Remak bundles was also lower in KO nerves 4 weeks after injury, although there was no difference in number of Remak after 8 weeks between WT and P2X₇ KO. Additionally, the Remak bundles in regenerating KO nerves contained a lower number

of unmyelinated axons at both 4 and 8 weeks after injury. Interestingly, at 4 weeks during regeneration we found an increased number of single unmyelinated axons (not belonging to Remak) in KO nerves compared to WT, with an inverted trend at 8 weeks. We believe that the increased number of single unmyelinated axons at 4 weeks is a feature of delayed re-myelination. Indeed, these axons could have been sorted for myelination, but yet to be myelinated. At 8 weeks following the repair the situation is inverted with a higher number of single unmyelinated axons in the WT compared to the controls. We can speculate that beside being delayed, myelination is also generally hindered in the absence of P2X7R. Indeed, this would explain the higher number of unmyelinated single axons in WT at 8 weeks, with a re-myelination program that is still active in WT mice, but delayed in P2X7 KO. The slower re-myelination profile in the KO mice is also further confirmed by the reduced number of myelinated axons at both 4 and 8 weeks, compared to WT. Overall, the radial sorting is a developmental physiologic process in which the Schwann cells choose mostly larger axons to myelinate. Radial sorting defects may occur in neuropathologic complications of the PNS. Interestingly, our observations corroborate the evidence that P2X7R might have a role in regulating the radial sorting process (Feltri *et al.*, 2016), as shown by the presence of structures composed of unmyelinated axons surrounding a myelinated fiber (electron micrographs), typical sign of morphological defects in radial sorting (Feltri *et al.*, 2016).

Furthermore, myelin thickness is lower in KO at 4 weeks; this is because the higher number of single unmyelinated (or lightly myelinated) axons causes the overall thinning of myelin thickness. This is further confirmation that myelination is delayed, together with the lower number of myelinated axons at both time points. Myelin thickness is higher in P2X7 KO nerves at 8 weeks. Similarly to what stated before, myelination is not only delayed in KO, but might also last less in general. Indeed, if this was the case the more active myelination program in WT would cause the overall myelin thickness to be lower at 8 weeks (due to an increased number of single unmyelinated/lightly myelinated axons still actively myelinating). Altogether, these complicated findings point towards the conclusion that re-myelination is delayed and globally hindered in the absence of P2X7 receptors.

In the acute phase following peripheral nerve injury, expression of P2X7R is upregulated in Schwann cells, which is associated with Schwann cell proliferation mediated by ATP (Song *et al.*, 2015). With respect to demyelinating neuropathies, Schwann cells taken from a rat model of Charcot-Marie-Tooth 1A show abnormally high intracellular Ca^{2+} concentration due to overexpression of P2X7R mediated by peripheral myelin protein 22 (PMP22). In this animal

model, the P2X7R reversible antagonist A438079 improved myelination in both *in vitro* organic DRG cultures, and *in vivo* histologic analysis. Consequentially these animals showed significant improvements in muscle strength and distal motor latencies compared to placebo controls, however compound muscle action potentials remained unaltered (Sociali *et al.*, 2016). Studies in rat Schwann cells have shown that exposure to high concentrations of ATP or P2X7R agonists (BzATP) induce significant rapid cell death, increasing membrane permeability to large molecules including ethidium. Furthermore, these responses were not seen with irreversible (oxaTP) or reversible (A438079) antagonists, or in P2X7R KO mice, therefore suggesting that P2X7R is responsible for ATP-induced Schwann cell death *in vitro* (Faroni *et al.*, 2013b; Luo *et al.*, 2013). Considering that ATP is present in high concentrations at the injury site, P2X7R is likely to be a mediator of Schwann cell death following injury.

Following nerve transection, structural proteins such as P0, PMP22, MAG and MBP are all rapidly downregulated (Mirsky & Jessen, 1999). On the contrary, neurotrophic factors such as NGF and BDNF are all upregulated, enabling axonal elongation and neuronal survival (Chen *et al.*, 2007). Neurotrophins, such as NGF and BDNF, are fundamental in the guidance of axonal elongation following peripheral nerve injury (Jessen & Mirsky, 2016). Interestingly, at T0 the P2X7 KO had a higher expression of all myelin proteins (i.e. P0, PMP22, MBP, MAG) compared to WT, corroborating the hypothesis of a strong correlation between the P2X7R and myelin proteins, and its involvement in nerve myelination (Nobbio *et al.*, 2009; Faroni *et al.*, 2014b). In this study, following 72 hours of *in vitro* degeneration, we successfully recapitulated several aspects of *in vivo* WD, including the downregulation of myelin proteins and the upregulation of neurotrophic growth factors (Faroni *et al.*, 2015). Moreover, 72 hours of *in vitro* WD also increased cell death, according to *in vivo* (Faroni *et al.*, 2015). Indeed, expression of both caspase 2 and caspase 3, which function as central regulators of cell death (D'Amelio *et al.*, 2010), increased after injury and *ex vivo* degeneration, suggesting that cell death is occurring.

Caspase 3 showed a higher degree of up-regulation in gene expression levels compared to caspase 2 in both WT and P2X7 KO nerves. Hanley *et al.* suggested that caspase 3 activation is ATP-concentration dependent and thus may be downstream of the P2X7R (Hanley *et al.*, 2012). Nevertheless, caspase 3 mediated cell death is independent of other apoptosis pathways, such as caspase-1 (Hanley *et al.*, 2012), and therefore other cell death mechanisms might be occurring. The activation of both caspase-3 and P2X7R is known to lead to membrane blebbing and subsequent cell death, via the degradation of cytoskeleton proteins (Janicke *et al.*, 1998).

Importantly, some of these changes also reflected on the DRGs, in which inflammatory mediators (e.g. NF κ B, TNF α , etc.) increased following nerve transection, both in WT and P2X7 KO. Gene expression changes in DRGs following peripheral nerve transection are part of the pathophysiological response of the PNS to nerve injury (Martin *et al.*, 2019). As NF κ B is ubiquitously expressed, the increase observed in the P2X7 KO may highlight an increased recruitment of inflammatory cells to the DRG, compared to the WT. Inflammation is required to clear the cellular debris and improve the environment for regeneration, however, it also increases cellular death and can counterbalance the recovery (Rock, 2009). Indeed, TNF is an apoptotic mediator, associated with a variety of other roles, including necrosis (Bradley, 2008), and DRG excitability determining neuropathic pain (Zhang *et al.*, 2007). The TNF α pro-apoptotic effect was also associated to up-regulation of caspase-2 and caspase-3, implying that an increase in cell death also occurred.

Nevertheless, in the DRGs we also found upregulation of factors that oppose the increase of cell death mediators, such as the transcription factor ATF3 or the neuropeptide galanin which are reported to improve neuronal survival after injury (Holmberg *et al.*, 2005; Hobson *et al.*, 2008). ATF3 is generally considered a marker of nerve injury, indeed naïve animals have a very low expression of ATF3 in the DRG neurons, while an injury induces its high upregulation (Tsujino *et al.*, 2000). Given that ATF3 has a role in controlling the expression of other genes that are important for recovery, it is one of the earliest genes to be upregulated following an injury (Hyatt Sachs *et al.*, 2007). Moreover, galanin upregulation after injury is also in accordance to data on injured superior cervical ganglia (Schreiber *et al.*, 1994). It is known that galanin is predominantly located in the small/medium neurons within the DRG, whereas P2X7R is mainly found in the surrounding glial cells, which suggests important functions for neuron-glia communication (Zhang *et al.*, 2007). Hence, in order to unveil the signalling cascade triggering the galanin gene expression increase, we hypothesized that the altered gene expression of galanin may be a result of the loss of this communication mechanism. Finally, we found that growth factors were upregulated in DRGs after injury, likely in order to promote axonal elongation. Indeed, it is well established that NGF is upregulated after injury in DRG (Lindsay, 1988; McMahon, 1996; Woolf & Costigan, 1999), and is vital for recovery of the DRG neurons (Lindsay, 1988). However, NGF exerts important roles in the neuroregenerative process as well as in the neuroinflammatory response within the adult DRG sensory neurons (McMahon, 1996; Woolf & Costigan, 1999). The

drop in NGF expression has also been correlated with the increase in galanin (Rao *et al.*, 1993; Shadiack *et al.*, 1998).

(Lindsay, 1988; McMahon, 1996; Woolf & Costigan, 1999) Collectively, our findings point to the role of P2X7R in the determination of Schwann cell fate, facilitating the transition of Schwann cells from immature to a myelinating phenotype (Figure 7). Namely, these receptors support the regeneration and re-myelination following peripheral nerve injury and in demyelinating neuropathies. More work needs to be done to understand the the role of P2X7R in non-myelinating Schwann cells, and to exploit P2X7 receptors as potential pharmacological targets for novel nerve repair strategies.

Acknowledgments

AF and AJR are supported by the Hargreaves and Ball Trust, the Academy of Medical Sciences (AMS-SGCL7), and by Seed Corn Funding from the Rosetrees Trust and the Stoneygate Trust (M746). We are grateful to Prof. Patrizia Procacci for the precious help in setting up the morphometric analysis and to Emily May Fisher for the analyses of the *ex vivo* model.

Abbreviations

Ach, Acetylcholine; ATF3, activating transcription factor 3; ATP, adenosine triphosphate; BDNF, brain derived neurotrophic factor; CASP2, caspase-2; CASP3, capsase-3; DRG, dorsal root ganglion; GABA, γ -aminobutyric acid; GAL, galanin; GAP43, growth associated protein 43; IC, circularity index ; MAG, myelin associated glycoprotein; MBP, myelin basic protein; NGF, nerve growth factor; P0, myelin protein zero; **P2X7R**, P2X purinergic receptor 7; PBS, phosphate buffered saline; TBST, tris-buffered saline-Tween; WD, Walerian degeneration; WT, wild type.

Data availability statement

The datasets generated during and/or analysed during the current study are available from the corresponding author on reasonable request.

Conflict of interest

The authors declare no competing financial or commercial interest.

Authors contribution

V.M., A.F., S.M, P.S., L.A. performed *in vivo* experiments, immunofluorescence and gene expression studies. V.C. and P.S. performed electron microscopy and image analysis. A.F. and A.J.R. did statistic. Study was designed by A.F., with assistance of V.M. and A.J.R. The manuscript written by V.M and A.F., with assistance of A.J.R.

References

- Allen-Jennings, A.E., Hartman, M.G., Kociba, G.J. & Hai, T. (2001) The roles of ATF3 in glucose homeostasis. A transgenic mouse model with liver dysfunction and defects in endocrine pancreas. *J Biol Chem*, **276**, 29507-29514.
- Bradley, J.R. (2008) TNF-mediated inflammatory disease. *J Pathol*, **214**, 149-160.
- Chen, Z.L., Yu, W.M. & Strickland, S. (2007) Peripheral regeneration. *Annu Rev Neurosci*, **30**, 209-233.
- Chessell, I.P., Hatcher, J.P., Bountra, C., Michel, A.D., Hughes, J.P., Green, P., Egerton, J., Murfin, M., Richardson, J., Peck, W.L., Grahames, C.B., Casula, M.A., Yiangou, Y., Birch, R., Anand, P. & Buell, G.N. (2005) Disruption of the P2X7 purinoceptor gene abolishes chronic inflammatory and neuropathic pain. *Pain*, **114**, 386-396.
- Cunningham, P.N., Dyanov, H.M., Park, P., Wang, J., Newell, K.A. & Quigg, R.J. (2002) Acute renal failure in endotoxemia is caused by TNF acting directly on TNF receptor-1 in kidney. *Journal of immunology*, **168**, 5817-5823.
- D'Amelio, M., Cavallucci, V. & Cecconi, F. (2010) Neuronal caspase-3 signaling: not only cell death. *Cell death and differentiation*, **17**, 1104-1114.
- Faroni, A., Calabrese, F., Riva, M.A., Terenghi, G. & Magnaghi, V. (2013a) Baclofen modulates the expression and release of neurotrophins in schwann-like adipose stem cells. *J Mol Neurosci*, **49**, 233-243.

Faroni, A., Castelnovo, L.F., Procacci, P., Caffino, L., Fumagalli, F., Melfi, S., Gambarotta, G., Bettler, B., Wrabetz, L. & Magnaghi, V. (2014a) Deletion of GABA-B receptor in Schwann cells regulates remak bundles and small nociceptive C-fibers. *Glia*, **62**, 548-565.

Faroni, A. & Magnaghi, V. (2011) The neurosteroid allopregnanolone modulates specific functions in central and peripheral glial cells. *Frontiers in endocrinology*, **2**, 103.

Faroni, A., Melfi, S., Castelnovo, L.F., Bonalume, V., Colleoni, D., Magni, P., Arauzo-Bravo, M.J., Reinbold, R. & Magnaghi, V. (2019) GABA-B1 Receptor-Null Schwann Cells Exhibit Compromised In Vitro Myelination. *Molecular neurobiology*, **56**, 1461-1474.

Faroni, A., Mobasser, S.A., Kingham, P.J. & Reid, A.J. (2015) Peripheral nerve regeneration: experimental strategies and future perspectives. *Adv Drug Deliv Rev*, **82-83**, 160-167.

Faroni, A., Rothwell, S.W., Grolla, A.A., Terenghi, G., Magnaghi, V. & Verkhratsky, A. (2013b) Differentiation of adipose-derived stem cells into Schwann cell phenotype induces expression of P2X receptors that control cell death. *Cell death & disease*, **4**, e743.

Faroni, A., Smith, R.J., Procacci, P., Castelnovo, L.F., Puccianti, E., Reid, A.J., Magnaghi, V. & Verkhratsky, A. (2014b) Purinergic signaling mediated by P2X7 receptors controls myelination in sciatic nerves. *J Neurosci Res*, **92**, 1259-1269.

Feltri, M.L., Poitelon, Y. & Previtali, S.C. (2016) How Schwann Cells Sort Axons: New Concepts. *Neuroscientist*, **22**, 252-265.

Fields, R.D. (2011) Nonsynaptic and nonvesicular ATP release from neurons and relevance to neuron-glia signaling. *Semin Cell Dev Biol*, **22**, 214-219.

Fields, R.D. & Burnstock, G. (2006) Purinergic signalling in neuron-glia interactions. *Nat Rev Neurosci*, **7**, 423-436.

Fields, R.D., Dutta, D.J., Belgrad, J. & Robnett, M. (2017) Cholinergic signaling in myelination. *Glia*, **65**, 687-698.

Fields, R.D. & Stevens, B. (2000) ATP: an extracellular signaling molecule between neurons and glia. *Trends Neurosci*, **23**, 625-633.

Fields, R.D. & Stevens-Graham, B. (2002) New insights into neuron-glia communication. *Science*, **298**, 556-562.

Gesing, A., Wang, F., List, E.O., Berryman, D.E., Masternak, M.M., Lewinski, A., Karbownik-Lewinska, M., Kopchick, J.J. & Bartke, A. (2015) Expression of apoptosis-related genes in liver-specific growth hormone receptor gene-disrupted mice is sex dependent. *J Gerontol A Biol Sci Med Sci*, **70**, 44-52.

Hanley, P.J., Kronlage, M., Kirschning, C., del Rey, A., Di Virgilio, F., Leipziger, J., Chessell, I.P., Sargin, S., Filippov, M.A., Lindemann, O., Mohr, S., Konigs, V., Schillers, H., Bahler, M. & Schwab, A. (2012) Transient P2X7 receptor activation triggers macrophage death independent of Toll-like receptors 2 and 4, caspase-1, and pannexin-1 proteins. *J Biol Chem*, **287**, 10650-10663.

Hanoux, V., Pairault, C., Bakalska, M., Habert, R. & Livera, G. (2007) Caspase-2 involvement during ionizing radiation-induced oocyte death in the mouse ovary. *Cell death and differentiation*, **14**, 671-681.

He, B., Counts, S.E., Perez, S.E., Hohmann, J.G., Koprach, J.B., Lipton, J.W., Steiner, R.A., Crawley, J.N. & Mufson, E.J. (2005) Ectopic galanin expression and normal galanin

receptor 2 and galanin receptor 3 mRNA levels in the forebrain of galanin transgenic mice. *Neuroscience*, **133**, 371-380.

Hobson, S.A., Bacon, A., Elliot-Hunt, C.R., Holmes, F.E., Kerr, N.C., Pope, R., Vanderplank, P. & Wynick, D. (2008) Galanin acts as a trophic factor to the central and peripheral nervous systems. *Cell Mol Life Sci*, **65**, 1806-1812.

Holmberg, K., Kuteeva, E., Brumovsky, P., Kahl, U., Karlstrom, H., Lucas, G.A., Rodriguez, J., Westerblad, H., Hilke, S., Theodorsson, E., Berge, O.G., Lendahl, U., Bartfai, T. & Hokfelt, T. (2005) Generation and phenotypic characterization of a galanin overexpressing mouse. *Neuroscience*, **133**, 59-77.

Hyatt Sachs, H., Schreiber, R.C., Shoemaker, S.E., Sabe, A., Reed, E. & Zigmond, R.E. (2007) Activating transcription factor 3 induction in sympathetic neurons after axotomy: response to decreased neurotrophin availability. *Neuroscience*, **150**, 887-897.

Janicke, R.U., Sprengart, M.L., Wati, M.R. & Porter, A.G. (1998) Caspase-3 is required for DNA fragmentation and morphological changes associated with apoptosis. *J Biol Chem*, **273**, 9357-9360.

Jessen, K.R. & Mirsky, R. (2016) The repair Schwann cell and its function in regenerating nerves. *J Physiol*, **594**, 3521-3531.

Lecca, D., Ceruti, S., Fumagalli, M. & Abbracchio, M.P. (2012) Purinergic trophic signalling in glial cells: functional effects and modulation of cell proliferation, differentiation, and death. *Purinergic signalling*, **8**, 539-557.

Lindsay, R.M. (1988) Nerve growth factors (NGF, BDNF) enhance axonal regeneration but are not required for survival of adult sensory neurons. *J Neurosci*, **8**, 2394-2405.

Accepted Article

Loreti, S., Ricordy, R., De Stefano, M.E., Augusti-Tocco, G. & Tata, A.M. (2007) Acetylcholine inhibits cell cycle progression in rat Schwann cells by activation of the M2 receptor subtype. *Neuron glia biology*, **3**, 269-279.

Loreti, S., Vilaro, M.T., Visentin, S., Rees, H., Levey, A.I. & Tata, A.M. (2006) Rat Schwann cells express M1-M4 muscarinic receptor subtypes. *J Neurosci Res*, **84**, 97-105.

Luo, J., Lee, S., Wu, D., Yeh, J., Ellamushi, H., Wheeler, A.P., Warnes, G., Zhang, Y. & Bo, X. (2013) P2X7 purinoceptors contribute to the death of Schwann cells transplanted into the spinal cord. *Cell death & disease*, **4**, e829.

Magnaghi, V., Ballabio, M., Camozzi, F., Colleoni, M., Consoli, A., Gassmann, M., Lauria, G., Motta, M., Procacci, P., Trovato, A.E. & Bettler, B. (2008) Altered peripheral myelination in mice lacking GABAB receptors. *Mol Cell Neurosci*, **37**, 599-609.

Magnaghi, V., Castelnovo, L.F., Faroni, A., Cavalli, E., Caffino, L., Colciago, A., Procacci, P. & Pajardi, G. (2014) Nerve regenerative effects of GABA-B ligands in a model of neuropathic pain. *Biomed Res Int*, **2014**, 368678.

Magnaghi, V., Procacci, P. & Tata, A.M. (2009) Chapter 15: Novel pharmacological approaches to Schwann cells as neuroprotective agents for peripheral nerve regeneration. *Int Rev Neurobiol*, **87**, 295-315.

Martin, S.L., Reid, A.J., Verkhatsky, A., Magnaghi, V. & Faroni, A. (2019) Gene expression changes in dorsal root ganglia following peripheral nerve injury: roles in inflammation, cell death and nociception. *Neural Regen Res*, **14**, 939-947.

Martinez de Albornoz, P., Delgado, P.J., Forriol, F. & Maffulli, N. (2011) Non-surgical therapies for peripheral nerve injury. *Br Med Bull*, **100**, 73-100.

Mayhew, T.M. & Sharma, A.K. (1984) Sampling schemes for estimating nerve fibre size. I. Methods for nerve trunks of mixed fascicularity. *Journal of anatomy*, **139 (Pt 1)**, 45-58.

McMahon, S.B. (1996) NGF as a mediator of inflammatory pain. *Philos Trans R Soc Lond B Biol Sci*, **351**, 431-440.

Mirsky, R. & Jessen, K.R. (1999) The neurobiology of Schwann cells. *Brain pathology*, **9**, 293-311.

Nagajyothi, F., Desruisseaux, M.S., Machado, F.S., Upadhyaya, R., Zhao, D., Schwartz, G.J., Teixeira, M.M., Albanese, C., Lisanti, M.P., Chua, S.C., Jr., Weiss, L.M., Scherer, P.E. & Tanowitz, H.B. (2012) Response of adipose tissue to early infection with *Trypanosoma cruzi* (Brazil strain). *J Infect Dis*, **205**, 830-840.

Namsolleck, P., Boato, F., Schwengel, K., Paulis, L., Matho, K.S., Geurts, N., Thone-Reineke, C., Lucht, K., Seidel, K., Hallberg, A., Dahlof, B., Unger, T., Hendrix, S. & Steckelings, U.M. (2013) AT2-receptor stimulation enhances axonal plasticity after spinal cord injury by upregulating BDNF expression. *Neurobiol Dis*, **51**, 177-191.

Nobbio, L., Sturla, L., Fiorese, F., Usai, C., Basile, G., Moreschi, I., Benvenuto, F., Zocchi, E., De Flora, A., Schenone, A. & Bruzzone, S. (2009) P2X7-mediated increased intracellular calcium causes functional derangement in Schwann cells from rats with CMT1A neuropathy. *J Biol Chem*, **284**, 23146-23158.

Rao, M.S., Sun, Y., Vaidyanathan, U., Landis, S.C. & Zigmond, R.E. (1993) Regulation of substance P is similar to that of vasoactive intestinal peptide after axotomy or explantation of the rat superior cervical ganglion. *Journal of neurobiology*, **24**, 571-580.

Rock, K.L. (2009) Pathobiology of inflammation to cell death. *Biol Blood Marrow Transplant*, **15**, 137-138.

Schreiber, R.C., Hyatt-Sachs, H., Bennett, T.A. & Zigmond, R.E. (1994) Galanin expression increases in adult rat sympathetic neurons after axotomy. *Neuroscience*, **60**, 17-27.

Shadiack, A.M., Vaccariello, S.A., Sun, Y. & Zigmond, R.E. (1998) Nerve growth factor inhibits sympathetic neurons' response to an injury cytokine. *Proc Natl Acad Sci U S A*, **95**, 7727-7730.

Sim, J.A., Young, M.T., Sung, H.Y., North, R.A. & Surprenant, A. (2004) Reanalysis of P2X7 receptor expression in rodent brain. *J Neurosci*, **24**, 6307-6314.

Sociali, G., Visigalli, D., Prukop, T., Cervellini, I., Mannino, E., Venturi, C., Bruzzone, S., Sereda, M.W. & Schenone, A. (2016) Tolerability and efficacy study of P2X7 inhibition in experimental Charcot-Marie-Tooth type 1A (CMT1A) neuropathy. *Neurobiol Dis*, **95**, 145-157.

Solle, M., Labasi, J., Perregaux, D.G., Stam, E., Petrushova, N., Koller, B.H., Griffiths, R.J. & Gabel, C.A. (2001) Altered cytokine production in mice lacking P2X(7) receptors. *J Biol Chem*, **276**, 125-132.

Song, X.M., Xu, X.H., Zhu, J., Guo, Z., Li, J., He, C., Burnstock, G., Yuan, H. & Xiang, Z. (2015) Up-regulation of P2X7 receptors mediating proliferation of Schwann cells after sciatic nerve injury. *Purinergic signalling*, **11**, 203-213.

Stevens, B. & Fields, R.D. (2000) Response of Schwann cells to action potentials in development. *Science*, **287**, 2267-2271.

Stevens, B., Porta, S., Haak, L.L., Gallo, V. & Fields, R.D. (2002) Adenosine: a neuron-glia transmitter promoting myelination in the CNS in response to action potentials. *Neuron*, **36**, 855-868.

Stevens, B., Tanner, S. & Fields, R.D. (1998) Control of myelination by specific patterns of neural impulses. *J Neurosci*, **18**, 9303-9311.

Tsujino, H., Kondo, E., Fukuoka, T., Dai, Y., Tokunaga, A., Miki, K., Yonenobu, K., Ochi, T. & Noguchi, K. (2000) Activating transcription factor 3 (ATF3) induction by axotomy in sensory and motoneurons: A novel neuronal marker of nerve injury. *Mol Cell Neurosci*, **15**, 170-182.

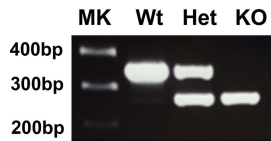
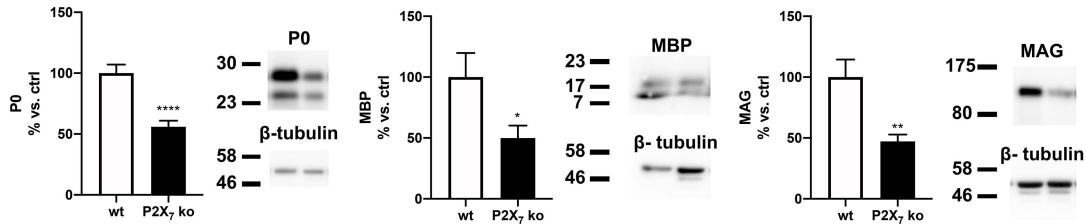
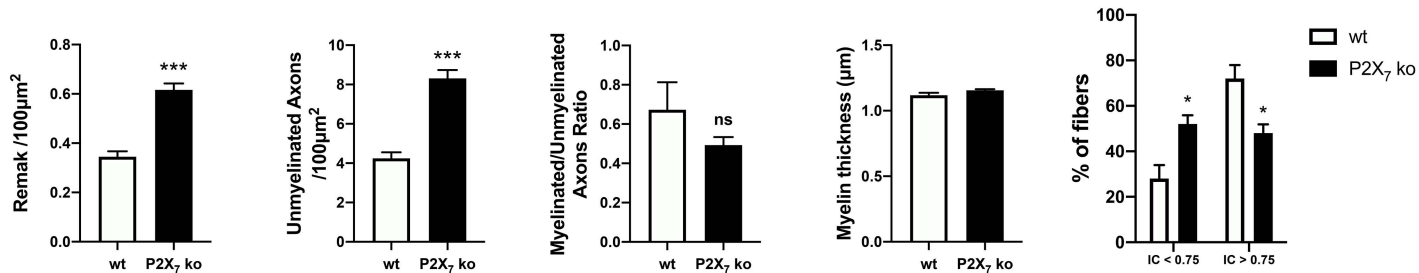
Uggetti, C., De Stefano, M.E., Costantino, M., Loreti, S., Pisano, A., Avallone, B., Talora, C., Magnaghi, V. & Tata, A.M. (2014) M2 muscarinic receptor activation regulates Schwann cell differentiation and myelin organization. *Dev Neurobiol*, **74**, 676-691.

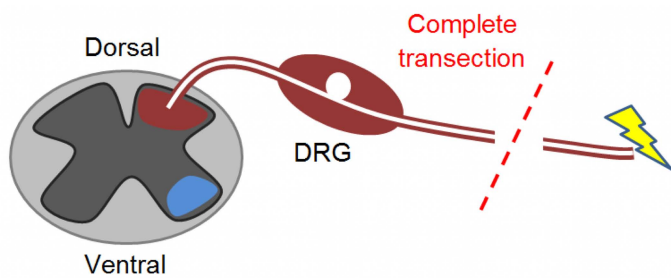
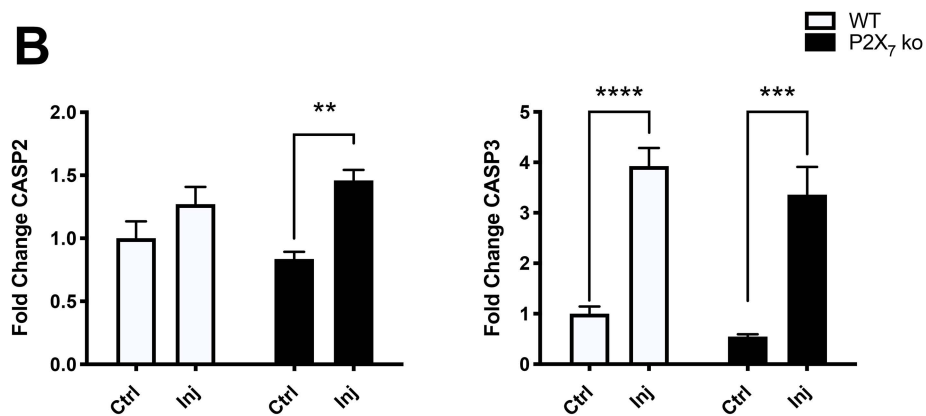
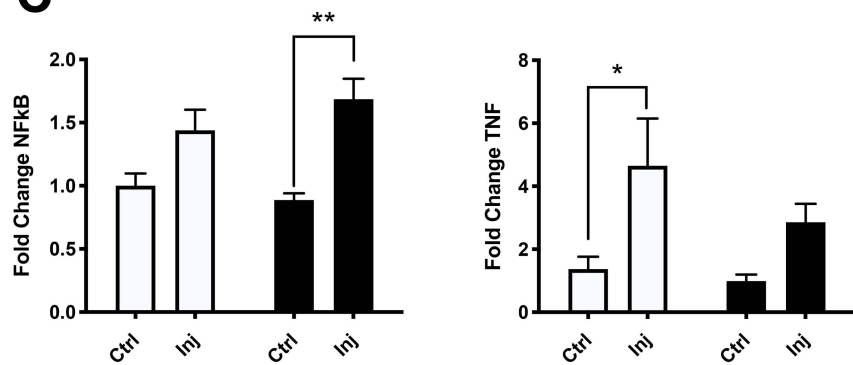
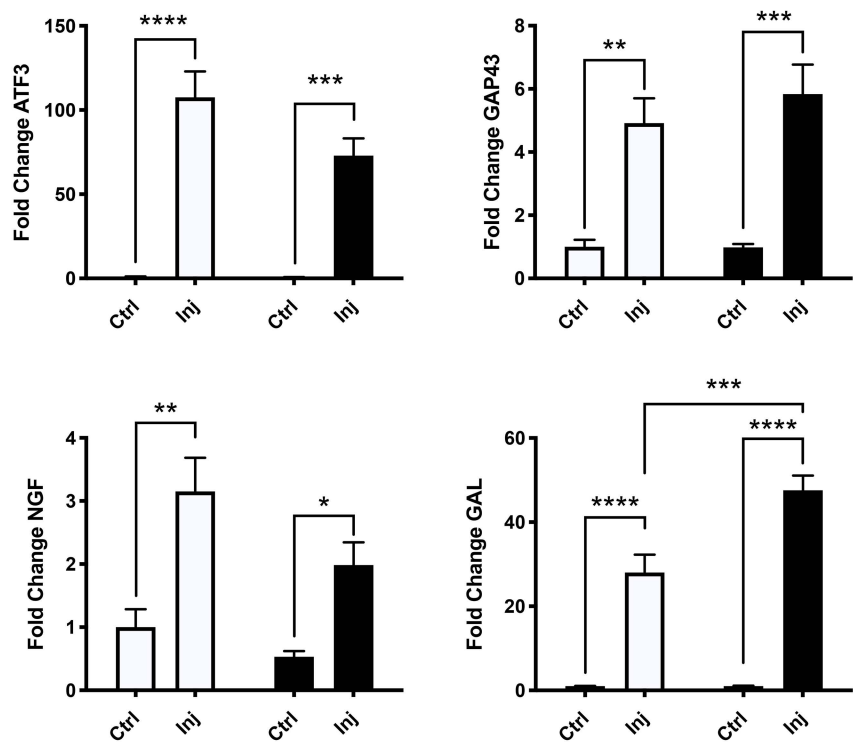
Verkhatsky, A., Krishtal, O.A. & Burnstock, G. (2009) Purinoceptors on neuroglia. *Molecular neurobiology*, **39**, 190-208.

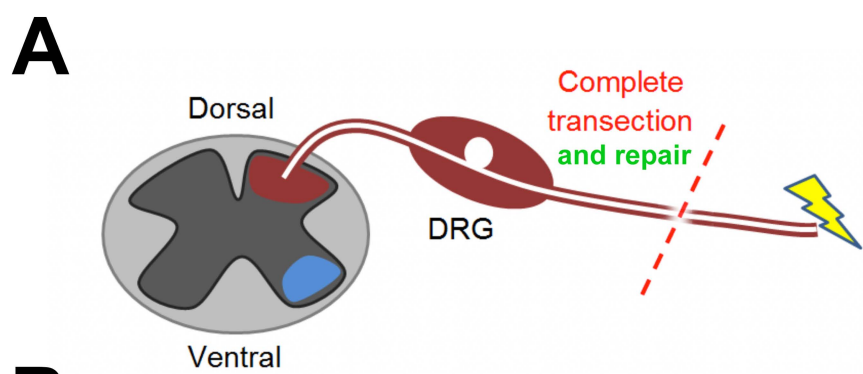
Woolf, C.J. & Costigan, M. (1999) Transcriptional and posttranslational plasticity and the generation of inflammatory pain. *Proc Natl Acad Sci U S A*, **96**, 7723-7730.

Zhang, X., Chen, Y., Wang, C. & Huang, L.Y. (2007) Neuronal somatic ATP release triggers neuron-satellite glial cell communication in dorsal root ganglia. *Proc Natl Acad Sci U S A*, **104**, 9864-9869.

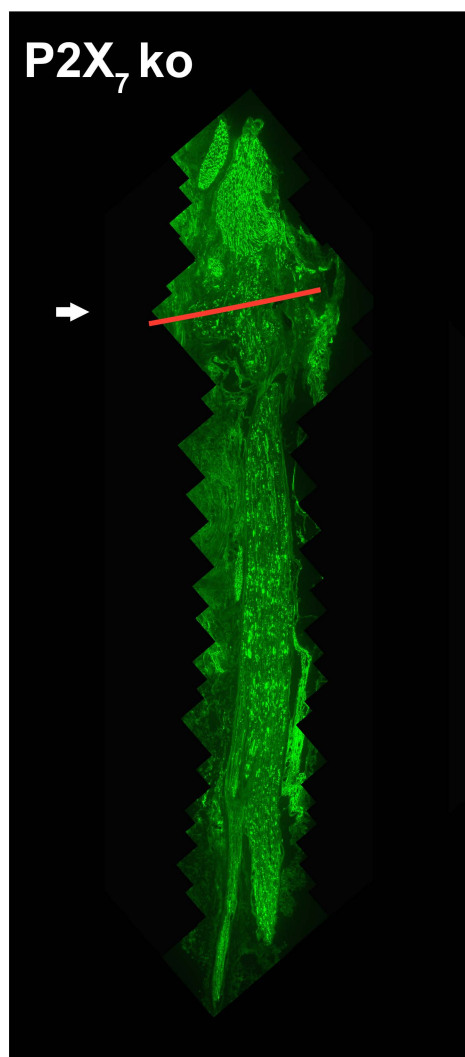
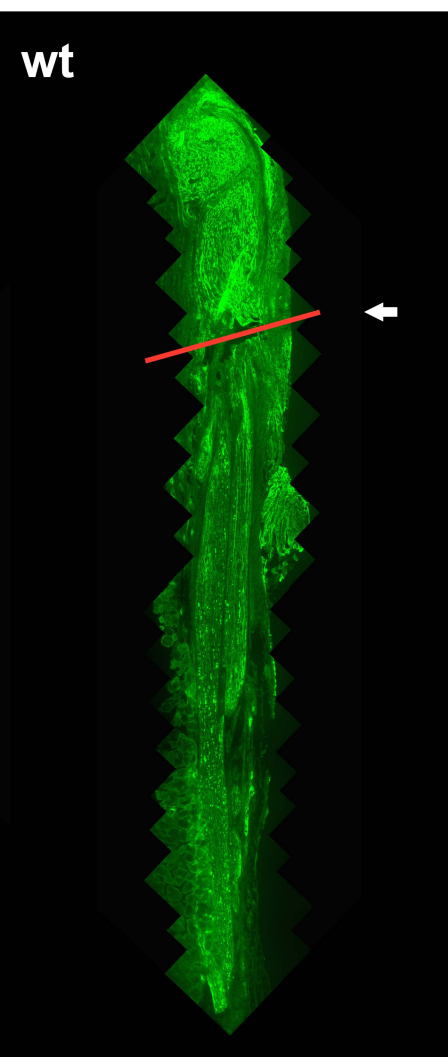
Zochodne, D.W. (2012) The challenges and beauty of peripheral nerve regrowth. *Journal of the peripheral nervous system : JPNS*, **17**, 1-18.

A**B****C**

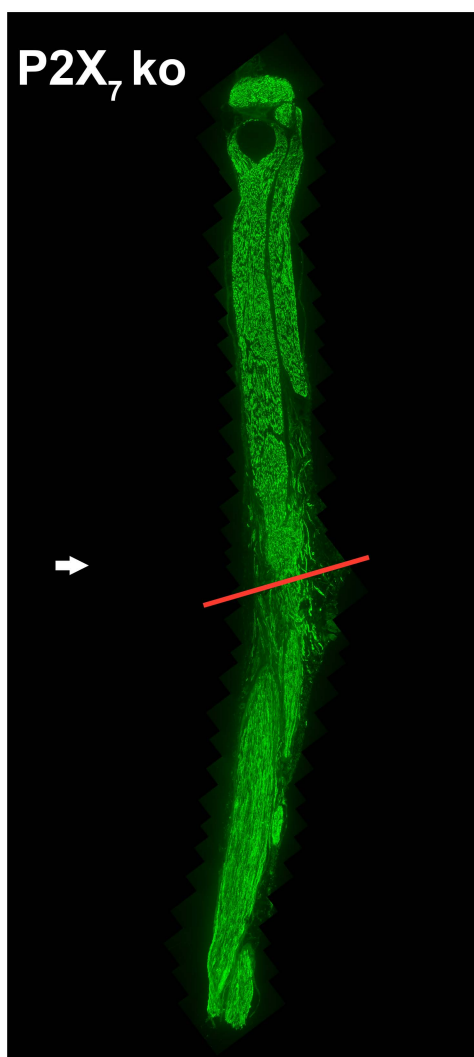
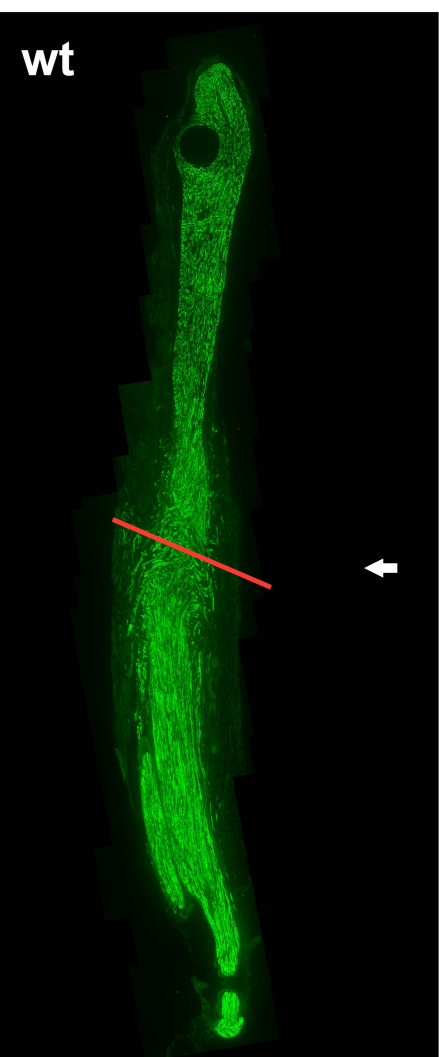
A**B****C****D**

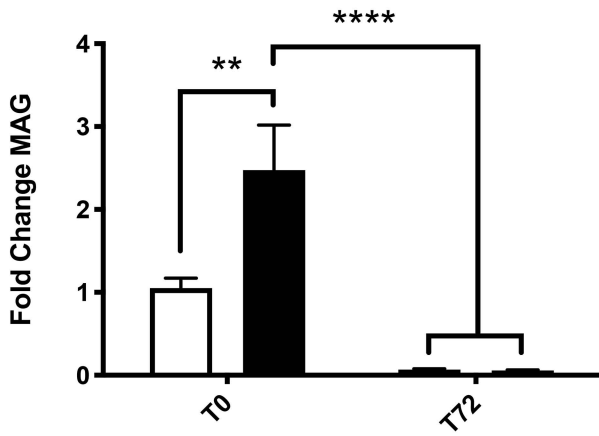
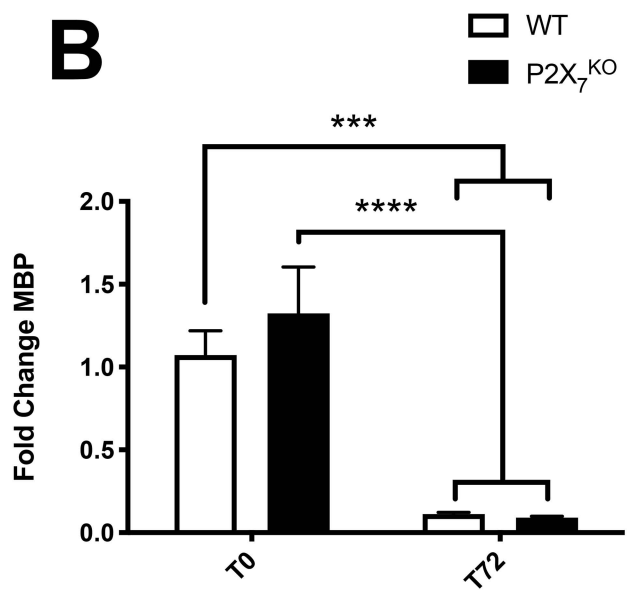
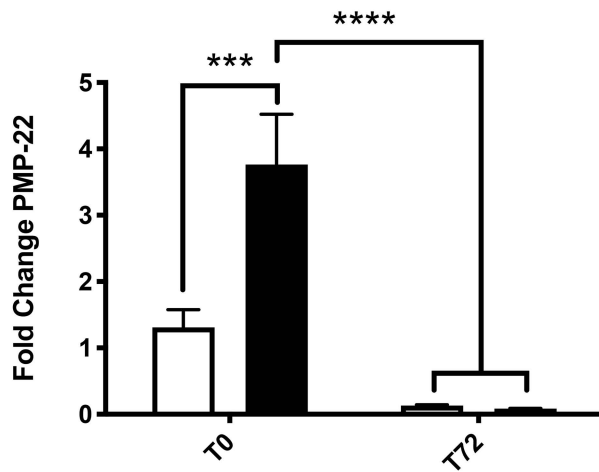
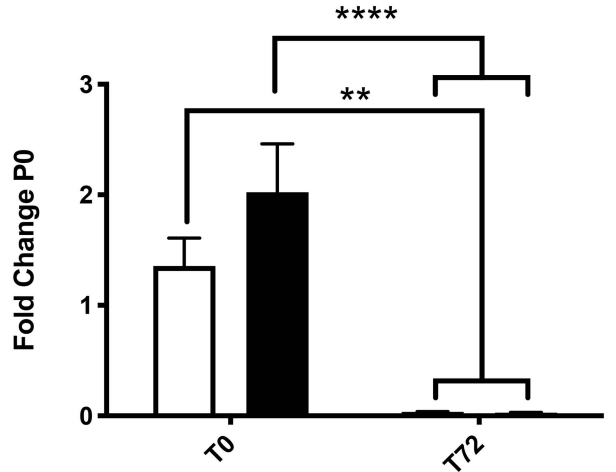
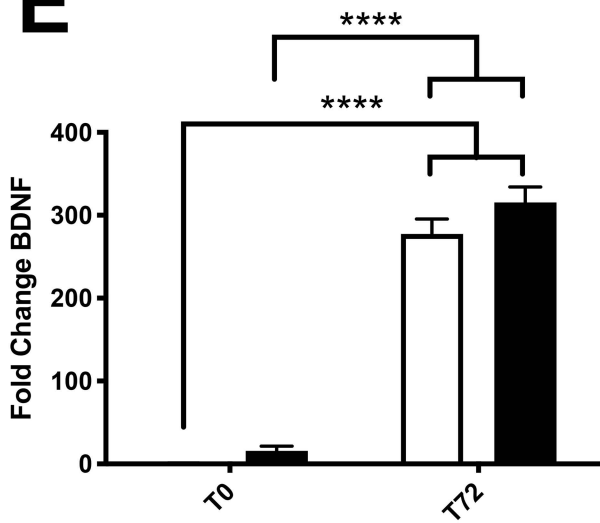
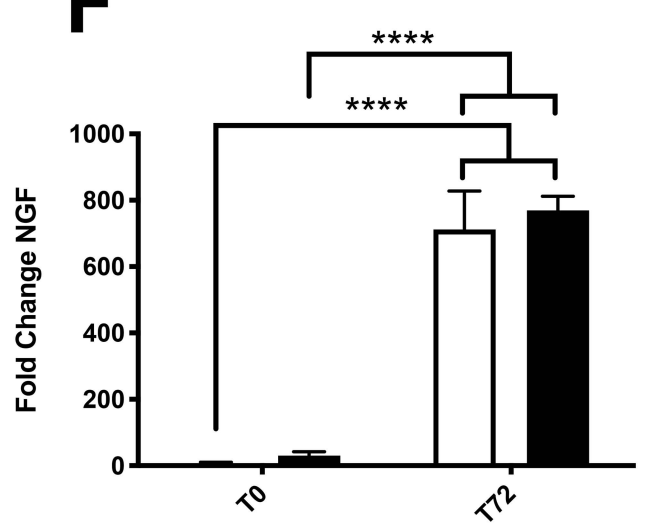
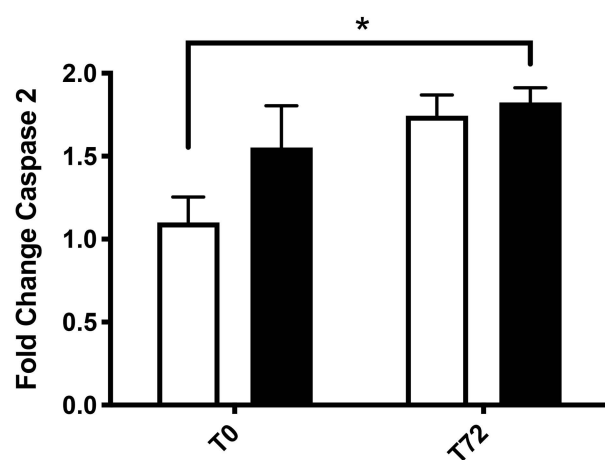
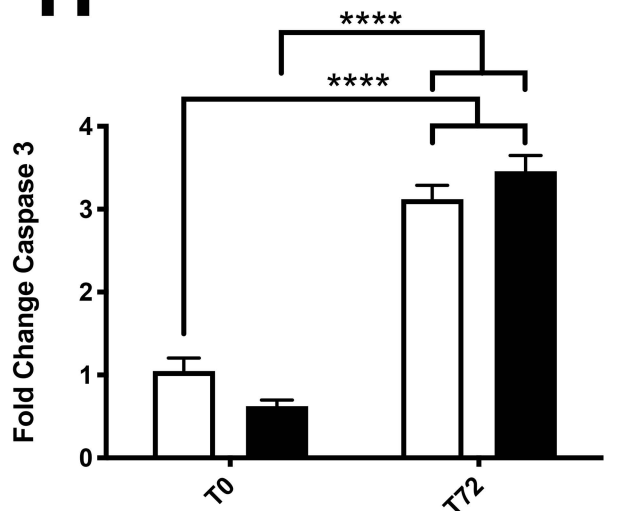


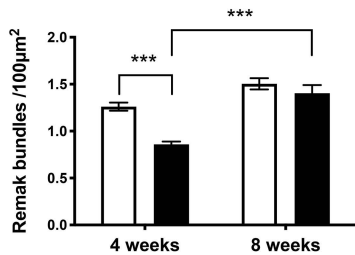
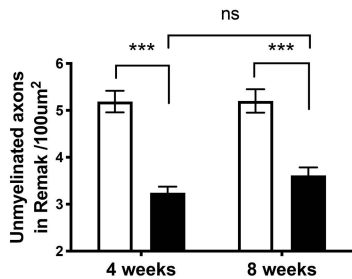
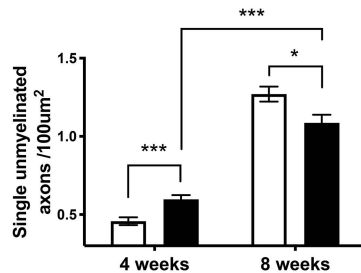
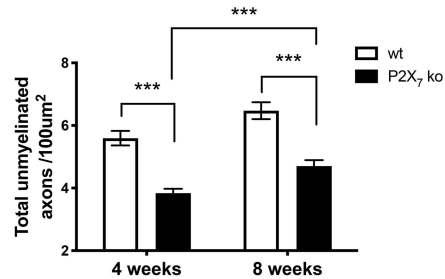
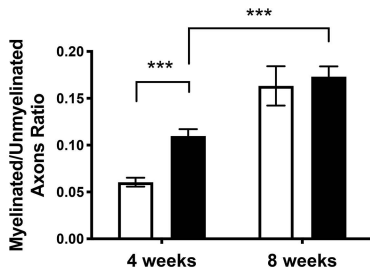
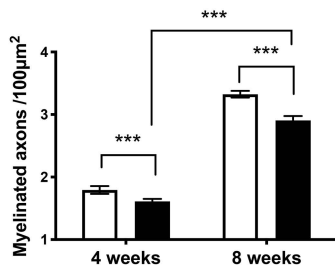
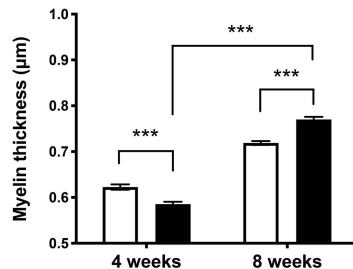
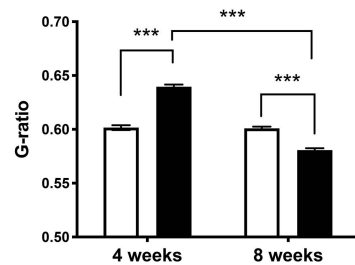
B



C



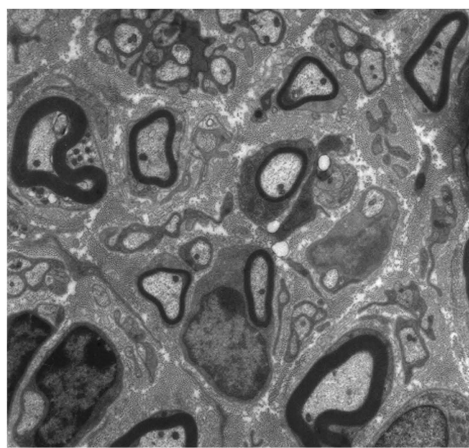
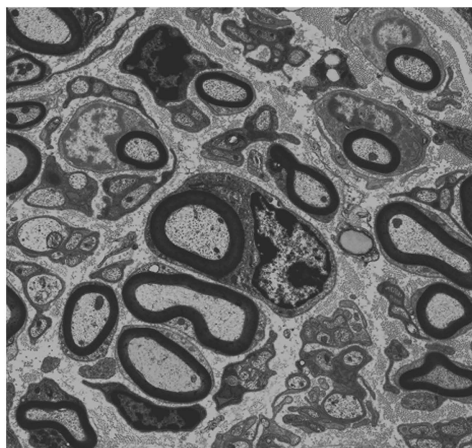
A**B****C****D****E****F****G****H**

A**B****C****D****E****F****G****H**

WT

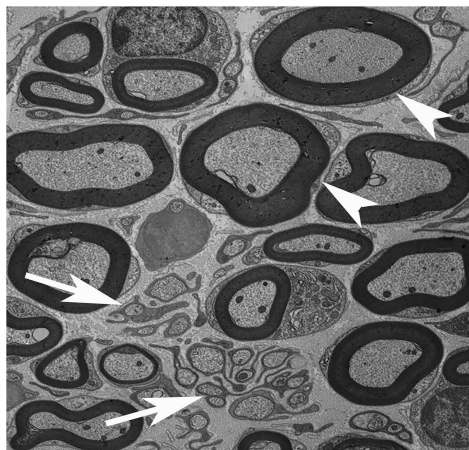
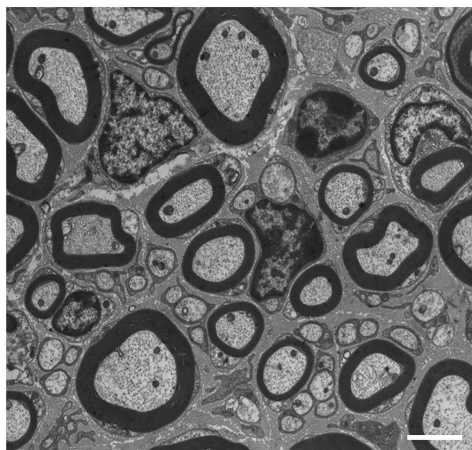
P2X₇ KO

4 weeks

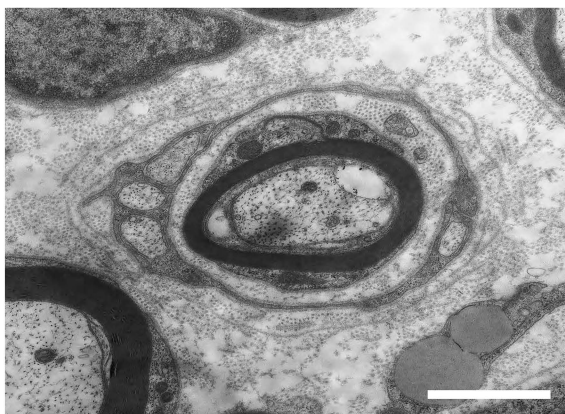


A

8 weeks



B



C

